Controlled polarization of two-dimensional quantum turbulence in atomic Bose-Einstein condensates

A. Cidrim,[1,2] F. E. A. dos Santos,[3] L. Galantucci,[2] V. S. Bagnato,[1] and C. F. Barenghi[2]

[1]*Instituto de Física de São Carlos, Universidade de São Paulo, Caixa Postal 369, 13560-970 São Carlos, São Paulo, Brazil*

[2]*JQC (Joint Quantum Centre Durham-Newcastle) and School of Mathematics and Statistics, Newcastle University, Newcastle upon Tyne, NE1 7RU, United Kingdom*

[3]*Departamento de Física, Universidade Federal de São Carlos, 13565-905, São Carlos, SP, Brazil*

(Received 11 July 2015; revised manuscript received 18 January 2016; published 30 March 2016)

We propose a scheme for generating two-dimensional turbulence in harmonically trapped atomic condensates with the novelty of controlling the polarization (net rotation) of the turbulence. Our scheme is based on an initial giant (multicharged) vortex which induces a large-scale circular flow. Two thin obstacles, created by blue-detuned laser beams, speed up the decay of the giant vortex into many singly quantized vortices of the same circulation; at the same time, vortex-antivortex pairs are created by the decaying circular flow past the obstacles. Rotation of the obstacles against the circular flow controls the relative proportion of positive and negative vortices, from the limit of strongly anisotropic turbulence (almost all vortices having the same sign) to that of isotropic turbulence (equal number of vortices and antivortices). Using this scheme, we numerically study the decay of two-dimensional quantum turbulence as a function of the polarization. Finally, we present a model for the decay rate of the vortex number which fits our numerical experiment curves, with the novelty of taking into account polarization time dependence.

DOI: 10.1103/PhysRevA.93.033651

I. INTRODUCTION

The study of quantum turbulence is heavily motivated by liquid helium (^{4}He and ^{3}He) experiments [1,2]. A striking discovery has been that, under appropriate forcing, quasiclassical behavior arises displaying statistical properties characteristic of ordinary turbulence; an example is the celebrated Kolmogorov $-\frac{5}{3}$ scaling of the energy spectrum [3] which suggests the existence of a classical energy cascade from large to small length scales. Under other conditions, a different kind of turbulence (called "ultraquantum turbulence" or "Vinen turbulence") has also been found [4,5], characterized by random tangles of vortices without large-scale, energy-containing flow structures. Quantum turbulence experiments are also performed in atomic Bose-Einstein condensates [6–9]; the relative small size of these condensates (compared to flows of liquid helium or of ordinary fluids) limits the study of scaling laws but offers opportunities to study minimal processes that also take place in larger systems (e.g., vortex interactions, vortex reconnections, vortex clustering) with greater experimental controllability and more direct visualization than in liquid helium.

Atomic condensates are also ideal systems to study two-dimensional (2D) turbulence [10], a problem with important applications to oceans, planetary atmospheres, and astrophysics. In classical systems, reduced dimensionality may arise from strong anisotropy, stratification, or rotation (via the Taylor-Proudman theorem). From the physicist's point of view, the dynamics of 2D turbulence is very different from three dimensional (3D) [11]. The existence (besides the kinetic energy) of a second inviscid quadratic invariant, the enstrophy, implies that a downscale enstrophy transfer is accompanied by an upscale energy cascade; in other words, in 2D turbulent flows the energy flows from small to large length scales rather than vice versa as in 3D turbulence. With the possible exception of soap films [12], 2D flows which can be created in the laboratory are only approximations. However, using suitable trapping potentials, atomic condensates can be easily shaped so that vortex dynamics is 2D rather than 3D. Unlike liquid helium, in atomic condensates 2D quantum vortices can be directly imaged, and, unlike classical systems, the motion of such 2D vortices is not hindered by viscous effects or friction with the substrate.

Several works have explored the generation of turbulence in 2D condensates. The 2D energy spectrum and scaling laws have been computed in numerical simulations [13–15], and the problem of what should be the quantum analog of the classical enstrophy has been raised. In Ref. [9], vortices were nucleated by small-scale stirring of a laser spoon, after which a persistent current was verified both experimentally and through numerical simulations, suggesting transfer of incompressible kinetic energy from small to large length scales. Emergence of large-scale order from vortex turbulence was also observed [16] as predicted by the "vortex gas" theory of Onsager. A similar setup was used to explore vortex shedding and annihilation processes in both experiments [17,18] and simulations [19]. The effect of stirring laser beams with different shapes or along different paths was investigated in Refs. [20–23]. However, in all cases cited, vortices have always been generated in such a way that the number of positive and negative vortices is approximately the same; in other words, all vortex configurations which have been investigated had approximately zero polarization. Since irrotational flow is a hallmark property of superfluidity, the polarization of the vortex configuration (i.e., the relative proportion of positive and negative vortices) plays the role of net rotational angular velocity Ω of a classical fluid, so it is important to explore its effects on the properties of turbulence.

In this work, we propose a scheme for generating 2D quantum turbulence in atomic condensates. Our scheme, which is based on a giant vortex as the initial state, is control over polarization of the turbulence, which can be interpreted as the

classical rotation of the entire flow. One of the most important properties of turbulence is its decay because the growth of the turbulence or its character in a steady state may depend on how it is forced, whereas the decay is an intrinsic property of the dynamics. We shall report the decay of 2D quantum turbulence as a function of the polarization.

II. GIANT VORTEX AND SMALL PINS

Multicharged vortices with circulations as large as 60 quanta have already been produced in condensates using dynamical methods, as consequences of rapid rotations of the confining trap [24]. Another route to achieve these highly excited states is using phase-engineering techniques, such as those described in Refs. [25–28]. In these cases, quanta of angular momentum are added to the condensate by adiabatically inverting the direction of the magnetic bias field which composes the usual Ioffe-Pritchard magnetic trap. To date, only charges below 10 quanta were produced using their proposed setups. However, an improvement on the method, known as the "vortex pump," has been described in Refs. [29–31]. In practical terms, a hexapole magnetic field is superposed to the Ioffe-Pritchard magnetic trap, allowing vorticity to be cyclically pumped into the condensate, thus generating giant vortices. Progress in this direction has been made in recent experiments with synthetic magnetic monopoles [32].

A giant vortex at the center of a harmonically trapped condensate can be described by a single-particle wave function of the form $\psi(\mathbf{r}) = f(r)e^{i\kappa\phi}$, where $f(r)$ is the wave function's amplitude, $\mathbf{r} = (r,\phi,z)$ is the position in cylindrical coordinates, and a large winding number κ corresponds to a large angular momentum. Such giant vortices are dynamically unstable [30,33], and split into singly quantized ($\kappa = 1$) vortices. Being parallel to one another, these singly quantized vortices impose a strongly azimuthal flow to the condensate. During the following evolution, some vortices of the opposite polarity may be generated by occasional large-amplitude density waves, but these events are rare, and do not change the main property of the flow resulting from the decay of a giant vortex configuration: the strong polarization of the vorticity (almost all vortices have the same sign).

The scheme that we propose uses blue-detuned lasers [18] to perturb this initial state with two diametrically opposite laser beams, creating thin obstacles (which we refer to as pins) with width σ of the order of magnitude of the healing length ξ (two pins are enough to homogenize the vortex distribution). The pins perturb the initial giant vortex, accelerating its decay; they also deflect the large azimuthal flow, generating vortex-antivortex pairs [19,34–36]. To control the effect of the pins, we move them at constant angular velocity ω in the direction opposite to the main azimuthal flow.

III. MODEL

The dynamics of our system is dictated by the 2D Gross-Pitaevskii equation (GPE). We introduce dimensionless variables based on the trapping potential of frequency ω_0, measuring times, distances, and energies in units of $\omega_0^{-1}, \sqrt{\hbar/m\omega_0}$, and $\hbar\omega_0$, respectively, where m is the mass of one atom and $\hbar$ is the reduced Planck's constant. The resulting dimensionless GPE is

$$i\frac{\partial\psi}{\partial t} = \left(-\frac{1}{2}\nabla^2 + V + C|\psi|^2 - \mu\right)\psi, \qquad (1)$$

where the time-dependent wave function $\psi(\mathbf{r},t)$ is normalized so that $\int|\psi|^2 d^2r = 1$. The external potential is $V(\mathbf{r},t) = V_{\rm trap}(\mathbf{r}) + V_{\rm pins}(\mathbf{r},t)$, where $V_{\rm trap}(\mathbf{r}) = (x^2+y^2)/2$ and $V_{\rm pins}(\mathbf{r},t) = V_+(\mathbf{r},t) + V_-(\mathbf{r},t)$ represent, respectively, the trapping potential which confines the condensates and the pins which perturb the initial giant vortex. The terms $V_\pm(\mathbf{r},t) = V_0\exp\{-|\mathbf{r}-\mathbf{r}_\pm(t)|^2/2\sigma^2\}$ with $\mathbf{r}_\pm(t) = [\pm x_0\cos(\omega t), y_0\sin(\omega t)]$ are diametrically opposite, thin, Gaussian potentials of width $\sigma = \xi$ which rotate clockwise (against the flow of the initially imposed giant vortex) at constant angular velocity ω. The quantity $C = 2\sqrt{2\pi}N(a/a_z)$ parametrizes the two-body collisions between the atoms, where N is the total number of atoms, a the scattering length, and a_z the axial harmonic oscillator's length; we choose $C = 17\,300$. The chemical potential μ is introduced to guarantee normalization of the wave function, and the amplitude of the pins is $V_0 \approx 1.43\mu$. In homogeneous systems ($V = 0$) the healing length is found by balancing kinetic and interaction energies terms in the GPE. In a harmonically trapped condensate, the healing length can be defined with reference to the density at the center of the trapped condensate in the absence of any vortex or hole. In our dimensionless units, we obtain $\xi \approx 0.13$, and $r_{\rm TF} \approx 74\xi$ for the Thomas-Fermi radius.

Our choice of dimensionless parameters corresponds to typical [17,18] experiments with ^{23}Na condensates (scattering length $a = 2.75$ nm, atom mass $m = 3.82\times10^{-26}$ kg) with $N = 1.3\times10^6$ atoms, radial and axial trapping frequencies $\omega_0 = 2\pi\times 9$ Hz and $\omega_z = 2\pi\times 400$ Hz, radial and axial harmonic oscillator's lengths $a_0 = \sqrt{\hbar/m\omega_0} \approx 7.1$ μm and $a_z = \sqrt{\hbar/m\omega_z} \approx 1.0$ μm, for which the dimensional healing length is $\xi = 0.13a_0 \approx 0.9$ μm; the laser beam would then have a Gaussian $1/e^2$ radius of $w_0 = 2\sigma \approx 1.8$ μm. Blue-detuned Gaussian laser beams have been used as pins in a series of experiments with highly oblate BECs [18,23,37]. Particularly in [37], a laser beam of width $w_0 \approx 2$ μm was used to stir a 2D ^{87}Rb condensate, similarly to what we propose, maintaining a circular motion with the help of piezodriven mirrors.

In order to define our initial state, a circulation of 37 quanta (i.e., winding number $\kappa = 37$) is initially imprinted around the center of the Thomas-Fermi profile, thus imposing an initial counterclockwise circular flow. Changing t into $-it$ in Eq. (1), we shortly evolve the state for $t = 0.09$ in imaginary-time description, guaranteeing a fixed phase of $2\pi\kappa$ in the center of the condensate and adjusting the density to the presence of the pins. We then compute the evolution in real time.

By substituting $t \to (1-i\gamma)t$ in Eq. (1), we are left with a phenomenological dissipative GPE (dGPE), where γ is a dissipation constant which models the interaction of the condensate with the surrounding thermal cloud. This equation can be used to investigate the effect of finite temperature in our system. With this aim, we also run simulations with the same initial states using dGPE instead of GPE. We choose $\gamma = 3.0\times10^{-4}$, a typical value of dissipative parameter [38–40], particularly chosen for the experimentally realistic case found

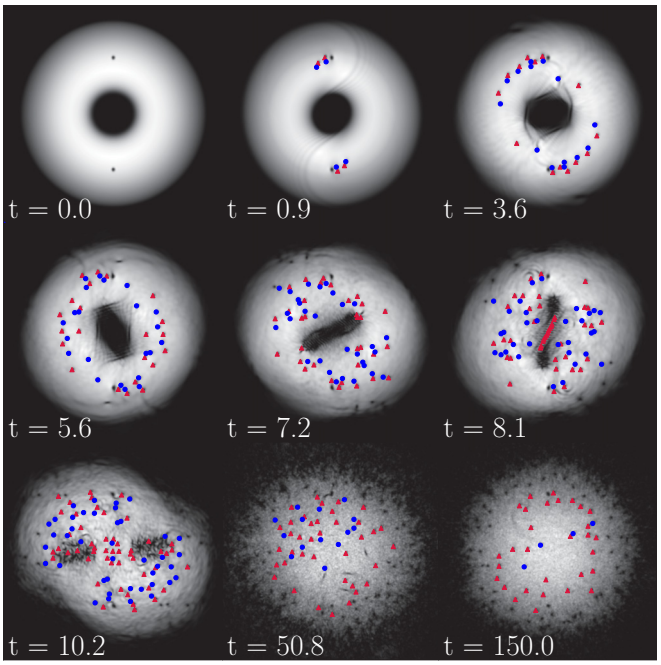

FIG. 1. Density plots of the condensate at different times t for $\omega = 0$ (nonrotating obstacles). Regions of large and low density are displayed in white and black, respectively. Red triangles and blue circles identify positive-charged and negative-charged vortices, respectively. The giant vortex decays by injecting a large number of singly quantized (positive) vortices into the condensate, while the pins generate vortex pairs, as can be clearly seen at time $t = 0.9$.

in current experiments [17,19]. Summarizing beforehand, we find the same overall behavior for both dissipationless and this specific dissipative case.

All numeric simulations are performed in the 2D domain $-25 \leqslant x, y \leqslant 25$ on a 512×512 grid using the fourth-order Runge-Kutta method in Fourier space with the help of XMDS [41].

IV. RESULTS

A. Creating polarized flow

We simulate the real-time evolution of the system for different values of the pins' angular velocity: $\omega = 0, \pi/16, \pi/8, \pi/6$, and $\pi/4$. A series of snapshots for the case of $\omega = 0$ is shown in Fig. 1 to exemplify a typical run. The initial large hole at the center of the figure is the core of the giant vortex. The two small holes (north and south of the giant hole) are the two stationary pins. The critical velocity v_c for the creation of a vortex-antivortex pair depends on the barrier's shape [19,42] and also on inhomogeneities of the system [18]. Typically, $v_c/c \sim 0.1$–0.4 for infinitely high cylindrical barriers, where c is the local speed of sound. Since our barriers (the pins) are either stationary or rotate against the main flow, vortex shedding is a dissipative mechanism which slows down the superfluid's azimuthal flow and removes angular momentum.

Aside from generating vortices of opposite sign, the pins act as a perturbation to the giant vortex and accelerate its decay process; for example, a wave front which perturbs the core of the giant vortex is visible at time $t = 0.9$ in Fig. 1. The decay of the giant vortex takes place via deformation of the core, which becomes elliptical before vanishing, and injecting a large number of positive, singly quantized vortices into the condensate. At the same time, vortex-antivortex pairs are created by the flow past the pins. This process continues until the large azimuthal flow is lower than the critical velocity v_c; at that point, the giant vortex has disappeared, and the pins are practically unable to generate further vortices. Therefore, after this slowdown and due to their small sizes, the pins are practically irrelevant to the vortex dynamics (apart from occasional creation of pairs in the fast rotating case, $\omega = \pi/4$). In spite of that, in order to study the vortex number decay, we simply remove them at $t = 82$ and allow for longer simulations.

We perform a phase-unwrapping procedure and, by detecting windings of $\pm 2\pi$ around small closed paths (plaquettes) on the phase profile [20], we are able to count the numbers N^+ and N^- of positive and negative singly quantized vortices in the system (anticlockwise and clockwise circulation, respectively). This vortex detection algorithm uses a density-cut criterion ($\sim$0.75 of $|\psi|^2$'s mean value) to avoid detection of ghost vortices. Given the initial giant vortex (which is multicharged and therefore not detected by our vortex-detecting algorithm), depending on the value of ω, there can be an imbalance of N^+ and N^- throughout the evolution. Vortices can be expelled from the condensate due to their mutual interaction, spiral out of the condensate because of dissipation, or undergo vortex-pair annihilation processes. In our particular finite-temperature simulation, we verify that the chosen experimentally realistic value of the dissipation parameter γ is small enough that, on the time scale analyzed (and compared to the dissipationless simulations), dissipation-induced spiraling out of individual vortices is less significant than vortex interactions or annihilations.

After the decay of the initial giant vortex, the imbalance of positive and negative vortices is measured by the polarization

$$P = \frac{(N^+ - N^-)}{(N^+ + N^-)} \tag{2}$$

which takes maximum or minimum values ($P = \pm 1$) if all vortices have positive or negative sign. Figure 2 shows the time evolution of the total number of vortices $N_{\rm tot}(t) = N^+ + N^-$ and of the polarization $P(t)$ under influence of the obstacles (present throughout the whole evolution) with angular velocity ω. Figure 2(a) shows that the maximum value of $N_{\rm tot}(t)$ increases with ω. It is apparent that, by choosing ω, we can control the polarization. We use this tunable mechanism to create initial vortex distributions (without the pins) as shown in Fig. 3, which plots $N_{\rm tot}(t)$ and $P(t)$ for initial states taken from instant $t = 82$ of Fig. 2. Clearly, by tuning ω we can produce a condensate free of external holes (the giant vortex or the obstacles) with approximately the desired vortex polarization.

By numerically detecting each vortex and its trajectory, we determine $N_{\rm tot}$ at each time step. By subtraction from the initial total vortex number $N_0 = N_{\rm tot}(0)$, we can infer the number of vortices which have drifted out of the condensate and the number of vortices which have disappeared in annihilation events, colliding with vortices of opposite sign. We find that such vortex-antivortex annihilation events generate density

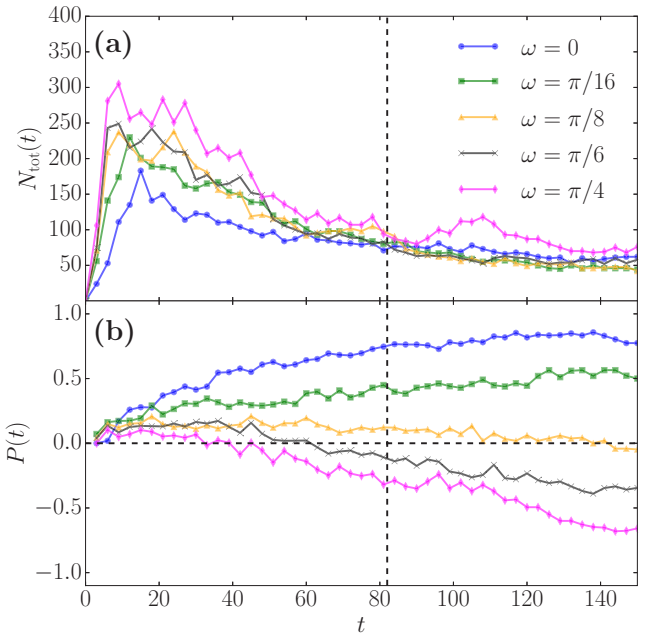

FIG. 2. (a) Total number of vortices N_{tot} vs time t; (b) polarization P vs time t. The vertical dashed line marks the time ($t = 82$) we use to make initial states for longer simulation without the pins. The curves are distributed in increasing value of ω from bottom to top, for the top plot, and conversely, for the bottom plot. In (a), at $t \approx 8$, from bottom to top, the curves refer, respectively, to $\omega = 0$, $\pi/16$, $\pi/8$, $\pi/6$, and $\pi/4$. In (b), from top to bottom, the curves refer, respectively, to the same latter series of increasing values of ω.

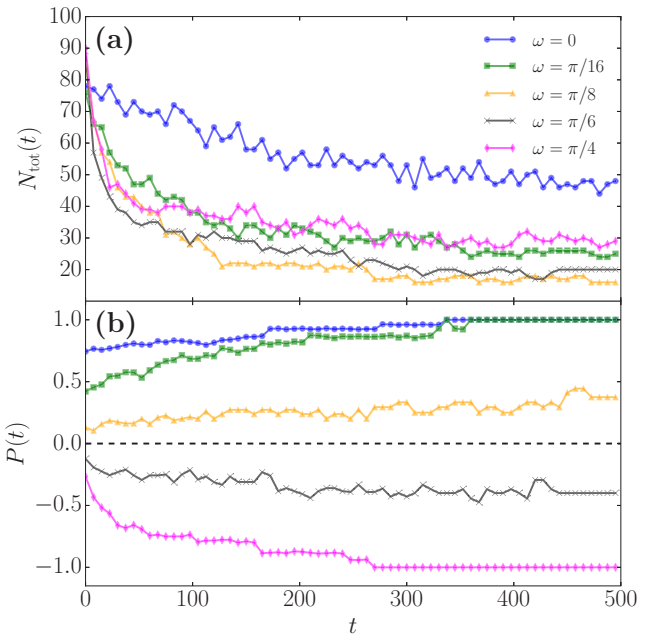

FIG. 3. (a) Total number of vortices N_{tot}; (b) polarization P vs time t, from initial states created at $t = 82$ in the previous stirring process (Fig. 2), labeled by the angular velocities which generated them. The pins are removed and we evolve those states longer in time to study the vortex number decay. In (a), at $t \approx 150$, from bottom to top, the curves refer, respectively, to $\omega = 0$, $\pi/4$, $\pi/16$, $\pi/6$, and $\pi/8$. In (b), from top to bottom, the curves are labeled as in Fig. 2(b).

waves, as already reported [19,43,44], turning incompressible energy into compressible energy. The reverse mechanism is also possible [45] and in our 2D case takes the form of vortex-antivortex creation events, which we observe. Creation events occur when the motion of the vortices induces a sufficiently deep density wave, or when a large amplitude wave approaches the edge of the condensate where the local speed of sound c is less than in the central region. We have also observed annihilation events immediately followed by creation events: this sequence happens when a vortex collides with an antivortex, producing a large sound wave, which almost immediately generates a new vortex-antivortex pair, due to the changing value of the local ratio v_c/c; this effect happens near the condensate's edge.

B. Polarized turbulence decay

Starting from $t > 82$ (when we remove the pins and start a new simulation), we examine whether there is a simple law for turbulence decay in 2D condensates. We remark that, consistently with previous work [17,19], in the time scales under investigation we do not observe a tendency to form large-scale clusters of vortices of the same sign, an effect called the inverse energy cascade in fluid dynamics and the negative temperature in the case of the Onsager gas of vortex points; the reason, as explained in a recent study [46], is the harmonic shape of the trapping potential. It has been suggested [17,19] that the decay rate of the total number of vortices is not exponential but can be phenomenologically described by the logistic equation

$$\frac{dN_{tot}}{dt} = -\Gamma_1 N_{tot} - \Gamma_2 N_{tot}^2, \tag{3}$$

where the linear term refers to vortex drifting out of the condensate, the nonlinear term arises from vortex-antivortex annihilation events, and the coefficients Γ_1 and Γ_2 are rates to be determined. We find that the solution of the logistic equation fits our decays for $t > 82$ (after pins removal) fairly well. However, in most cases which we examined, the fitting parameter Γ_1 is negative, corresponding to positive growth. Clearly, after the pins are removed, no vortex generation is expected (apart from occasional creation of vortex-antivortex pairs as mentioned above); therefore a naive association of the linear term of the logistic equation with vortex drifting out of the condensate does not seem appropriate.

In alternative to the logistic model of Eq. (3), we propose a model which captures some essential physics of the complex vortex interaction, although only in an idealized way. First, we model the rate of drift of vortices out of the condensate [attributed to the linear term of Eq. (3) in [17,19]]. Consider a positive vortex near the edge of the condensate. In the first approximation, its trajectory is a random zigzag caused by the other vortices (see Fig. 4). The azimuthal velocity component of the vortex v_θ will be biased by its sign and, hence, the (opposite) sign of its image with respect to the boundary of the condensate (in the present case of a positive vortex, the interaction with its negative image will give to v_θ an anticlockwise contribution). This azimuthal flow, however, gives no contribution to the vortex drift out of the condensate: what matters to the rate of vortex decay is only the radial

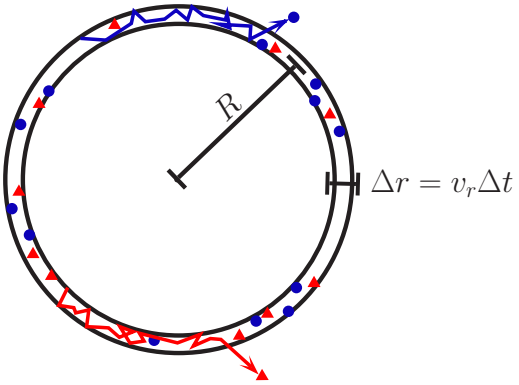

FIG. 4. Schematic trajectories of vortices in a thin annulus of thickness $\Delta r = v_r \Delta t$ near the edge of a condensate of radius R. Vortices (red triangles) and antivortices (blue dots) describe erratic paths (arrowed lines) due to interaction with other vortices. Collisions, mainly with same-signed vortices, drive vortices out of the condensate.

component v_r which will depend on the velocity induced by the surrounding vortices $\mathbf{v}_i$. In this simple model, $\mathbf{v}_i$ can be thought as the velocity induced by the nearest vortex located (if we consider a random vortex distribution) at the typical average inter-vortex distance $\ell \approx n^{-1/2}$, where $n = N/(\pi R^2)$ is the number of vortices per unit area (in 2D) or the length of vortex line per unit volume (in 3D) and N is the number of vortices in the condensate of radius R.[1]

[1]This scaling is well known in the superfluid helium literature, and has been numerically verified by D. Kivotides, Y. A. Sergeev, and C. F. Barenghi, Phys. Fluids **20**, 055105 (2008).

The magnitude of the induced velocity $\mathbf{v}_i$ will, hence, be approximately $v_i \approx \kappa/(2\pi\ell) = \kappa N^{1/2}/(2\pi^{3/2}R)$ (where $\kappa = \pm 1$ is the circulation in our units). The resulting radial velocity of the vortex v_r is therefore given by the expression $v_r \approx \beta v_i \approx \beta\kappa N^{1/2}/(2\pi^{3/2}R)$, where $|\beta| \leqslant 1$ depends on the direction of $\mathbf{v}_i$ and thus on the sign and the relative angular position of the nearest vortex.

Since collisions which take vortices out of the condensate are mainly with vortices of the same (positive) sign, we only use N^+ to estimate ℓ in this term, accounting for the polarization. In this idealized model, the number of positive vortices ΔN^+ expelled from the condensate in the (small) time Δt will therefore be proportional to the number of positive vortices N_a^+ lying in the small circular annulus of width $\Delta r = v_i \Delta t$ and area $\Delta A = 2\pi R \Delta r$, next to the edge of the condensate: these are the only positive vortices which can potentially travel a radial distance greater than their separation gap from the boundary of the condensate. Hence, assuming a uniform vortex distribution we have $\Delta N^+ \propto N_a^+ \approx N^+ \Delta A/(\pi R^2) = \kappa N^{+3/2} \Delta t/(\pi^{3/2} R^2)$. Taking the limit for small Δt, we conclude that positive vortices drift out of the condensate as $dN^+/dt \propto (N^+)^{3/2}$; similarly, $dN^-/dt \propto (N^-)^{3/2}$ for negative vortices.

We turn now the attention to the nonlinear term of Eq. (3), and remark that polarization must be included in the description. In Ref. [17], the authors added the nonlinear term on the intuitive assumption that annihilation rate depends on the number of vortex dipoles (composed of a positive and a negative vortex) which can be formed, which is of order $\propto N^2$ in a zero-polarized system. Following a similar reasoning, in a polarized system the annihilation rate should then be of order $\propto N^+ N^-$, as fewer vortex-dipole pairs are formed if $P \neq 0$

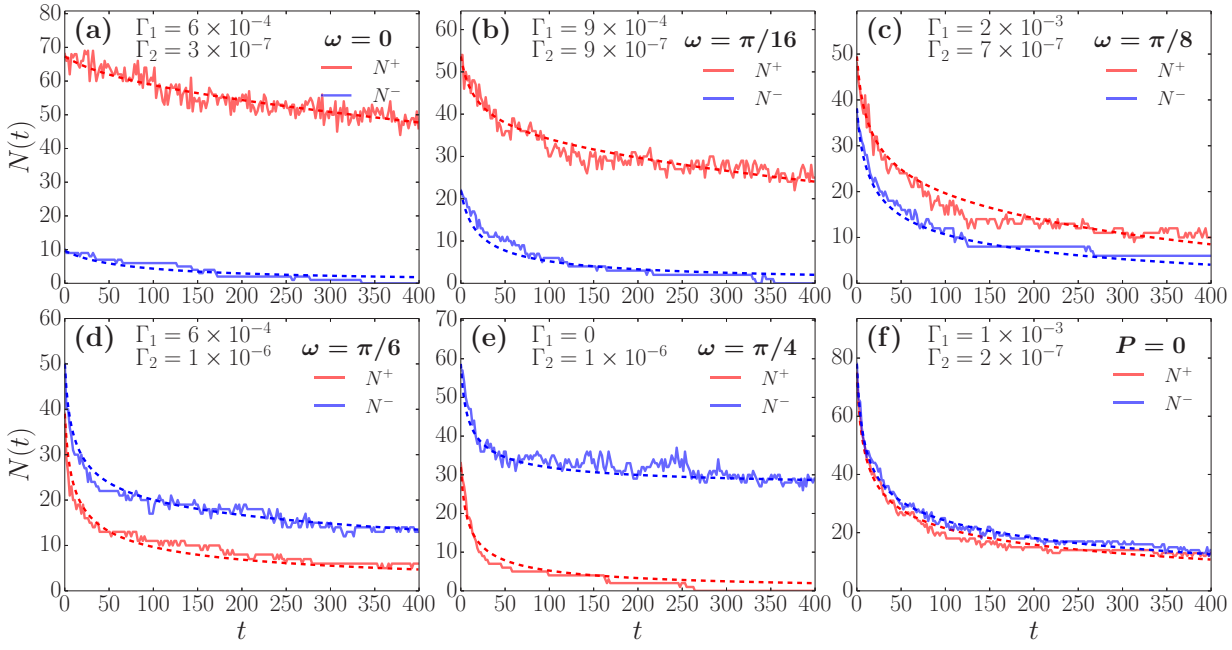

FIG. 5. Positive and negative vortex numbers N^+ and N^- decay as a function of time t for cases (a) $\omega = 0$; (b) $\omega = \pi/16$; (c) $\omega = \pi/8$; (d) $\omega = \pi/6$; (e) $\omega = \pi/4$; and (f) phase imprinted $P = 0$. The dashed lines are the respective fits for the numerical data (full lines) with the fitting parameters Γ_1 and Γ_2 appearing at top part of each plot. For plots (a), (b), and (c), the top and bottom curves are related to the positive and negative vortex numbers, respectively; for plots (d), (e), and (f), curves are in the opposite order.

(this consideration implicitly allows for any time dependence of the polarization).

We conclude that, in alternative to Eq. (3), a more physically realistic (although still rather idealized) model is

$$\begin{aligned}\frac{dN^+}{dt} &= -\Gamma_1(N^+)^{3/2} - \Gamma_2(N^+N^-)^2,\\ \frac{dN^-}{dt} &= -\Gamma_1(N^-)^{3/2} - \Gamma_2(N^+N^-)^2.\end{aligned} \tag{4}$$

Summing up Eqs. (4), the total number of vortices $N_{tot} = N^+ + N^-$ decays nontrivially as a function of polarization $P = P(t)$ according to

$$\frac{dN_{\rm tot}}{dt} = -\Gamma_1 f(t) N_{\rm tot}^{3/2} - \Gamma_2 g(t) N_{\rm tot}^4, \tag{5}$$

where the time-dependent polarization $P(t)$ appears in the functions

$$f(t) \equiv [(1+P)/2]^{3/2} + [(1-P)/2]^{3/2}, \tag{6}$$

$$g(t) \equiv (1-P^2)^2/8. \tag{7}$$

Notice that in our model the rates of drift and annihilation have, respectively, dependence $N_{\rm tot}^{3/2}$ and $N_{\rm tot}^4$ [rather than $N_{\rm tot}$ and $N_{\rm tot}^2$ of Eq. (3)]. The fit to the data is slightly better, and both coefficients Γ_1 and Γ_2 are positive (see Fig. 5), consistently with the interpretation of the two terms of the equation. Above all, our model is not arbitrary, but attempts to capture some of the physics of vortex interaction.

The same $N_{\rm tot}^4$ scaling for the annihilation rate was justified heuristically in the context of a quenched 2D homogeneous system in Ref. [47]. Recently, in Ref. [46], the $N_{\rm tot}^4$ scaling was also associated with a four-body process in simulations of trapped systems, in agreement with our observations. The general behavior is as follows: initially, a vortex dipole interacts with a third, catalyst vortex (or antivortex), turning into a rarefaction wave which the authors of Ref. [46] called a *vortexonium* in analogy with the positronium (the neutral bound state of an electron an a positron). The vortexonium travels through the condensate until it encounters a fourth vortex (or antivortex), which acts as a second catalyst. The four-body annihilation process is completed when the collision of the vortexonium with the fourth vortex converts the vortexonium irreversibly into sound. Figure 6 illustrates the process, showing zoomed-in images of a typical vortex-pair annihilation time sequence from our simulations. In this particular case, the third and fourth bodies are catalyst vortex and antivortex, respectively [see Figs. 6(c) and 6(f)]. It is important to notice that the process of vortex unbind that we have previously discussed often frustrates the last step of this process (i.e., the interaction with the second catalyst vortex) and the annihilation does not happen: although the vortexonium is formed, the local speed of sound may quickly change and split the dipole back again.

Vortex decay curves as a function of the polarization are shown in Fig. 5. We can identify cases (b) and (e) ($\omega = \pi/16$ and $\omega = \pi/4$), (c) and (d) ($\omega = \pi/8$ and $\omega = \pi/6$), respectively, as counterparts with the opposite polarization: the decay curves are similar in behavior, with mirror-symmetric polarization. The main difference between a curve and its

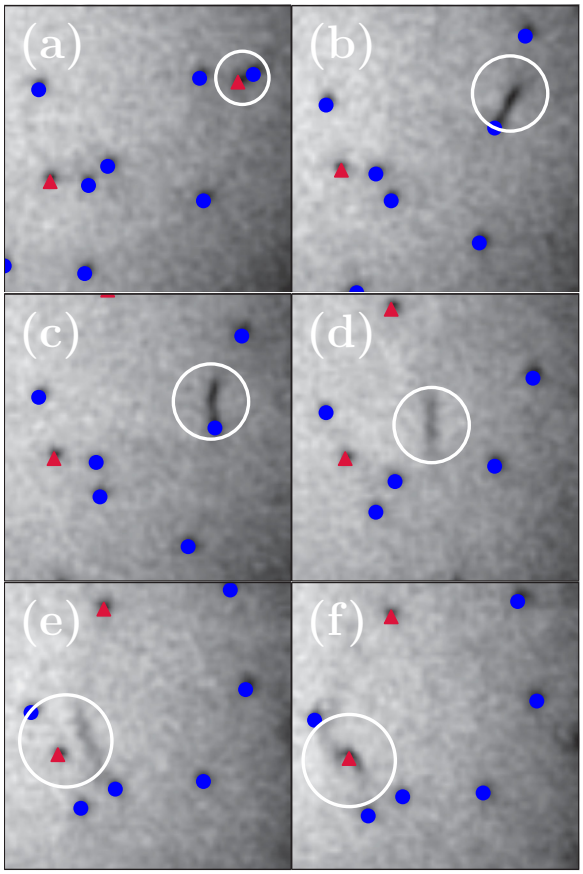

FIG. 6. Vortex annihilation through a four-body process. The white circles highlight the time sequence, which shows that (a) a vortex dipole is formed; (b) the dipole turns into a solitary wave (vortexonium) by interacting with a catalyst vortex; (c) the solitary wave deflects the catalyst vortex; (d) it travels to a higher density region, becoming a grayer, rarefaction pulse; (e) the pulse is about to collide with an anti-vortex; and (f) the annihilation process is complete after the collision, where the pulse is irreversibly converted into sound.

counterpart is the steeper number decay at initial times for (c) and (e). We found that the number of vortices lost due to annihilations is always considerably less than due to drift. Drift out of the condensate is strongly induced by vortex interactions: the values of the dissipation parameter γ which we used are too small to make vortices to spiral out of the condensate in the time scales studied. Therefore, both linear and nonlinear terms in Eq. (5) have origins in vortex interactions. Case (e) ($\omega = \pi/4$) illustrates well the need for a steeper than quadratic term in the rate equation since it characterizes a purely nonlinear decay (i.e., $\Gamma_1 = 0$).

Finally, in order to compare models from Eqs. (3) with (5) we performed numerical experiments in which, rather than creating vorticity with the giant vortex pins set up here proposed, we simply numerically imprint a given initial number of vortices uniformly at random positions onto the same harmonically trapped condensate. We obtain essentially the following results: the polarization approximately retains its initial value $P = 0$ [see Fig. 5(f)], and a reasonable fit is obtained using Eq. (3). As opposed to the polarized cases, we find non-negative rates. However, we see in the comparison

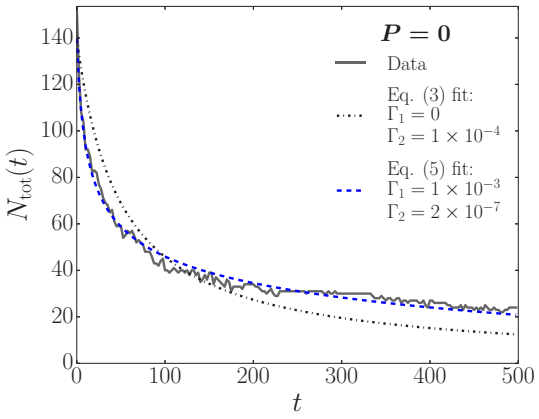

FIG. 7. Total number of vortices $N_{\rm tot}$ vs time t for the case where an unpolarized $P = 0$ vortex distribution was created through phase imprinting, in order to compare fits given by Eq. (3) (black dotted-dashed line) and Eq. (5) (blue dashed line).

shown in Fig. 4 that Eq. (5) fits the curve better than Eq. (3), clearly showing that the $\propto N^4$ scaling is a better fit than $\propto N^2$. Similarly to the polarized cases, drift is the main mechanism of vortex loss. Equation (3) has modeled well the decays studied by [17,19], which differs from our $P = 0$ case not in polarization but rather in the initial number of vortices ($\sim$60 as opposed to our $\sim$140) (see Fig. 7). Therefore, we attribute the departure from the quadratic decay (which is consistent with the "ultraquantum" decay observed [4,5] in superfluid helium, where the system's finiteness was not an issue) to vortex mutual interaction in a confined region. The finite-size system probably imposes a limit to the number of vortices which can be accommodated in the condensate.

In summary, for both polarized case and the particular unpolarized case where the vortex density is high, our rate equation (5) successfully describes the evolution of the total number of vortices.

V. CONCLUSION

We have presented a scheme for generating 2D quantum turbulence in atomic condensates which allows control over the polarization of the flow, equivalent to the net rotation of a turbulent ordinary fluid. Using this experimentally feasible scheme, we have examined the decay of the turbulence and the vortex interactions (vortex-antivortex creation and annihilation) which take place in the condensate. We have modeled the decay of the number of vortices using a rate equation that takes into account the time-dependent polarization. The rate equation (5) is physically more justified and gives a better fit to the numerical experiments than the logistic equation proposed by [17]; in particular, its two terms have clearly distinct physical meaning in terms of drift and annihilation. It also agrees with the recent finding of Ref. [46] in suggesting that vortex annihilation is a four-vortex process. The rate equation is therefore a better starting point to interpret the decay of 2D quantum turbulence in further experiments and simulations in which turbulence is generated in different ways, which will help understanding the scatter of the values of Γ_1 and Γ_2.

ACKNOWLEDGMENTS

We thank G. W. Stagg and A. J. Groszek for useful discussions, and W. J. Kwon and Y. Shin for insightful suggestion on the phenomenological model, particularly for proposing the inclusion of polarization in the vortex number rate equation as a nonlinear term $\propto N^+N^-$. This research was financially supported by CAPES (PDSE Proc. No. BEX 9637/14-1), CNPq, and FAPESP. L.G.'s work is supported by Fonds National de la Recherche, Luxembourg, Grant No. 7745104. The Núcleo de Apoio a Óptica e Fotônica (NAPOF-USP) is acknowledged for computational resources. This work made use of the facilities of N8 HPC Centre of Excellence, provided and funded by the N8 consortium and EPSRC (Grant No. EP/K000225/1).

[1] L. Skrbek and K. R. Sreenivasan, Phys. Fluids **24**, 011301 (2012).
[2] C. F. Barenghi, L. Skrbek, and K. R. Sreenivasan, Proc. Natl. Acad. Sci. USA, Suppl. **111**, 4647 (2014).
[3] C. F. Barenghi, V. S. L'vov, and P.-E. Roche, Proc. Natl. Acad. Sci. USA, Suppl. **111**, 4683 (2014).
[4] P. M. Walmsley and A. I. Golov, Phys. Rev. Lett. **100**, 245301 (2008).
[5] A. W. Baggaley, C. F. Barenghi, and Y. A. Sergeev, Phys. Rev. B **85**, 060501 (2012).
[6] M. C. Tsatsos, P. E. S. Tavares, A. Cidrim, A. R. Fritsch, M. A. Caracanhas, F. E. A. dos Santos, C. F. Barenghi, and V. S. Bagnato, Physics Reports **622**, 1 (2016).
[7] E. A. L. Henn, J. A. Seman, G. Roati, K. M. F. Magalhães, and V. S. Bagnato, Phys. Rev. Lett. **103**, 045301 (2009).
[8] E. A. L. Henn, J. A. Seman, G. Roati, K. M. F. Magalhães, and V. S. Bagnato, J. Low Temp. Phys. **158**, 435 (2009).
[9] T. W. Neely, A. S. Bradley, E. C. Samson, S. J. Rooney, E. M. Wright, K. J. H. Law, R. Carretero-González, P. G. Kevrekidis, M. J. Davis, and B. P. Anderson, Phys. Rev. Lett. **111**, 235301 (2013).
[10] A. C. White, B. P. Anderson, and V. S. Bagnato, Proc. Natl. Acad. Sci. USA, Suppl. **111**, 4719 (2014).
[11] R. H. Kraichnan and D. Montgomery, Rep. Prog. Phys. **43** 547 (1980).
[12] M. Rivera, P. Vorobieff, and R. E. Ecke, Phys. Rev. Lett. **81**, 1417 (1998).
[13] R. Numasato, M. Tsubota, and V. S. L'vov, Phys. Rev. A **81**, 063630 (2010).
[14] N. G. Parker and C. S. Adams, Phys. Rev. Lett. **95**, 145301 (2005).
[15] B. Nowak, D. Sexty, and T. Gasenzer, Phys. Rev. B **84**, 020506 (2011).
[16] T. Simula, M. J. Davis, and K. Helmerson, Phys. Rev. Lett. **113**, 165302 (2014).
[17] W. J. Kwon, G. Moon, J. Y. Choi, S. W. Seo, and Y.-i. Shin, Phys. Rev. A **90**, 063627 (2014).
[18] W. J. Kwon, G. Moon, S. W. Seo, and Y. Shin, Phys. Rev. A **91**, 053615 (2015).

[19] G. W. Stagg, A. J. Allen, N. G. Parker, and C. F. Barenghi, Phys. Rev. A **91**, 013612 (2015).
[20] A. C. White, C. F. Barenghi, and N. P. Proukakis, Phys. Rev. A **86**, 013635 (2012).
[21] M. T. Reeves, B. P. Anderson, and A. S. Bradley, Phys. Rev. A **86**, 053621 (2012).
[22] A. C. White, N. P. Proukakis, and C. F. Barenghi, J. Phys.: Conf. Ser. **544**, 012021 (2014).
[23] T. W. Neely, E. C. Samson, A. S. Bradley, M. J. Davis, and B. P. Anderson, Phys. Rev. Lett. **104**, 160401 (2010).
[24] P. Engels, I. Coddington, P. C. Haljan, V. Schweikhard, and E. A. Cornell, Phys. Rev. Lett. **90**, 170405 (2003).
[25] A. E. Leanhardt, A. Görlitz, A. P. Chikkatur, D. Kielpinski, Y. Shin, D. E. Pritchard, and W. Ketterle, Phys. Rev. Lett. **89**, 190403 (2002).
[26] M. Nakahara, T. Isoshima, and K. Machida, Phys. B (Amsterdam) **288**, 17 (2000).
[27] T. Isoshima, M. Okano, H. Yasuda, K. Kasa, J. A. M. Huhtamäki, M. Kumakura, and Y. Takahashi, Phys. Rev. Lett. **99**, 200403 (2007).
[28] M. Möttönen, N. Matsumoto, M. Nakahara, and T. Ohmi, J. Phys.: Condens. Matter **14**, 13481 (2002).
[29] M. Möttönen, V. Pietilä, and S. M. M. Virtanen, Phys. Rev. Lett. **99**, 250406 (2007).
[30] P. Kuopanportti and M. Möttönen, J. Low Temp. Phys. **161**, 561 (2010).
[31] P. Kuopanportti, B. P. Anderson, and M. Möttönen, Phys. Rev. A **87**, 033623 (2013).
[32] M. W. Ray, E. Ruokokoski, S. Kandel, M. Möttönen, and D. S. Hall, Nature (London) **505**, 657 (2014).
[33] P. Kuopanportti and M. Möttönen, Phys. Rev. A **81**, 033627 (2010).
[34] T. Frisch, Y. Pomeau, and S. Rica, Phys. Rev. Lett. **69**, 1644 (1992).
[35] T. Winiecki, J. F. McCann, and C. S. Adams, Europhys. Lett. **48**, 475 (1999).
[36] N. G. Berloff and P. H. Roberts, J. Phys. A: Math. Gen. **33**, 4025 (2000).
[37] R. Desbuquois, L. Chomaz, T. Yefsah, J. Léonard, J. Beugnon, C. Weitenberg, and J. Dalibard, Nat. Phys. **8**, 645 (2012).
[38] S. Choi, S. A. Morgan, and K. Burnett, Phys. Rev. A **57**, 4057 (1998).
[39] M. Tsubota, K. Kasamatsu, and M. Ueda, Phys. Rev. A **65**, 023603 (2002).
[40] A. S. Bradley and B. P. Anderson, Phys. Rev. X **2**, 041001 (2012).
[41] G. R. Dennis, J. J. Hope, and M. T. Johnsson, Comput. Phys. Commun. **184**, 201 (2013).
[42] F. Pinsker and N. G. Berloff, Phys. Rev. A **89**, 053605 (2014).
[43] M. Leadbeater, T. Winiecki, D. C. Samuels, C. F. Barenghi, and C. S. Adams, Phys. Rev. Lett. **86**, 1410 (2001).
[44] N. G. Parker, N. P. Proukakis, C. F. Barenghi, and C. S. Adams, Phys. Rev. Lett. **92**, 160403 (2004).
[45] N. G. Berloff and C. F. Barenghi, Phys. Rev. Lett. **93**, 090401 (2004).
[46] A. J. Groszek, T. P. Simula, D. M. Paganin, and K. Helmerson, arXiv:1511.06552 [Phys. Rev. A (to be published)].
[47] J. Schole, B. Nowak, and T. Gasenzer, Phys. Rev. A **86**, 013624 (2012).